

Effects of punctuated sediment supply on valley-floor landforms and sediment transport

Daniel J. Miller*

Lee E. Benda

Earth Systems Institute, 1314 North East 43rd Street, Seattle, Washington 98105, USA

ABSTRACT

Large, infrequent fluxes of sediment to streams by mass wasting are intrinsic to the erosion regime of mountain drainage basins. To elucidate the role of mass wasting in the construction and evolution of steep land channel environments, it is crucial that we identify the processes involved and recognize their legacy on the valley floor. In the winter of 1996, nine storm-triggered debris flows carried ~18 000 m³ of coarse debris into the upper reaches of the South Fork of Gate Creek (Oregon Cascade Range) during flood flow. Analysis of resulting channel morphologies and bed textures shows that the sediment moved downstream as a wave-like pulse or pulses, overwhelming the channel and causing it to braid, with flooding and alluvial deposition over the valley floor. Downstream progression of the sediment wave resulted in vertical accretion of the valley floor with sediment carried as bedload, the maximum depth of valley-floor burial being set by the amplitude of the wave. Passage of the wave left a channel incised to bedrock, inset between coarse-grained alluvial terraces. This study examines the genesis of these features at Gate Creek and points to such terraces as field indicators of massive episodic influxes of sediment and the associated formation of fluvially transported sediment waves.

Keywords: debris flow, fluvial transport, sediment supply, sediment transport, terraces.

INTRODUCTION

Episodes of mass wasting and surface erosion can rapidly deliver large quantities of

sediment to valley floors, which floods then rearrange into channel and riparian landforms. The morphology and textural composition of terraces, flood plains, and channel beds document the events that supply and move sediment, and provide indications of the frequency and magnitude with which they occur. Recognition of past event and process signatures can aid in assessing the potential for future channel change and in anticipating the consequences of large sediment influxes and floods. Unfortunately, such signs can be difficult to interpret, particularly for rare events that leave a lasting legacy but few clues as to their genesis.

In this study we examine channel and riparian landforms following such a high-supply event. A large storm in February 1996 triggered nine debris flows that carried ~18 000 m³ of coarse sediment into the upper reaches of the South Fork of Gate Creek, Oregon Cascade Range. Our observations indicate that this sediment traveled downstream as a coherent slug, i.e., a sediment wave. Arrival of the wave downstream caused channel aggradation and flooding of riparian areas and adjacent terraces. The channel widened and became braided. The passing of the wave left a channel incised to an immobile bed, inset between coarse-grained, alluvial terraces. Terraces gained a fresh veneer of gravel and numerous, newly excavated side channels.

Genesis of a downstream-moving wave of sediment at Gate Creek had profound geomorphic consequences. Had deposition occurred as a series of downstream-tapering wedges from the points of sediment entry, the total length of channel aggraded to a depth sufficient to bury and flood riparian areas would have been considerably less. Translation of the sediment as a coherent wave resulted in downstream aggradation to a consistently deep depth. The sediment wave caused overbank deposition of gravel-sized bedload

and accretion of the valley floor to extend kilometers downstream of the points of sediment entry.

Studies worldwide have documented wave-like transport of bed material following large sediment influxes. Wave lengths ranged from hundreds to thousands of meters and wave depths ranged from decimeters to several meters (Beschta, 1981; Gilbert, 1917; Griffiths, 1979; Madej and Ozaki, 1996; Meade, 1985; Nakamura, 1986; Pickup et al., 1983; Roberts and Church, 1986; Turner, 1995). Transient channel changes similar to those inferred at Gate Creek have been observed in many rivers following large sediment influxes and sediment-wave passage. These include (1) aggradation followed by incision (Gilbert, 1917; Griffiths, 1979; Pickup et al., 1983; Roberts and Church, 1986); (2) an increase in channel width followed by narrowing (Beschta, 1984; James, 1991); (3) fining of the channel-bed-surface-sediment grain size followed by coarsening (Coates and Collins, 1984; Meade, 1985; Roberts and Church, 1986); (4) transformation of single channels to braided channels (Roberts and Church, 1986); (5) decrease in the number of pools in conjunction with an increase in riffles followed by an increase in pool frequency and depth (Madej and Ozaki, 1996); (6) construction of terraces (Hack and Goodlett, 1960; Kochel et al., 1987; Nakamura, 1986; Roberts and Church, 1986; Turner, 1995); and (7) death of riparian forests (Everitt, 1968; Janda et al., 1975; Sigafos, 1964).

Sediment waves have been classified by volume (Nicholas et al., 1995) and studied in laboratory flumes (Gomez et al., 1989; Lisle et al., 1997). Mathematical models of wave-like sediment transport have been developed to reproduce field observations (Pickup et al., 1983; Weir, 1983). Simulation modeling has been used to investigate relationships between frequency and magnitude of mass wasting and

*E-mail: dan@ohana.org.

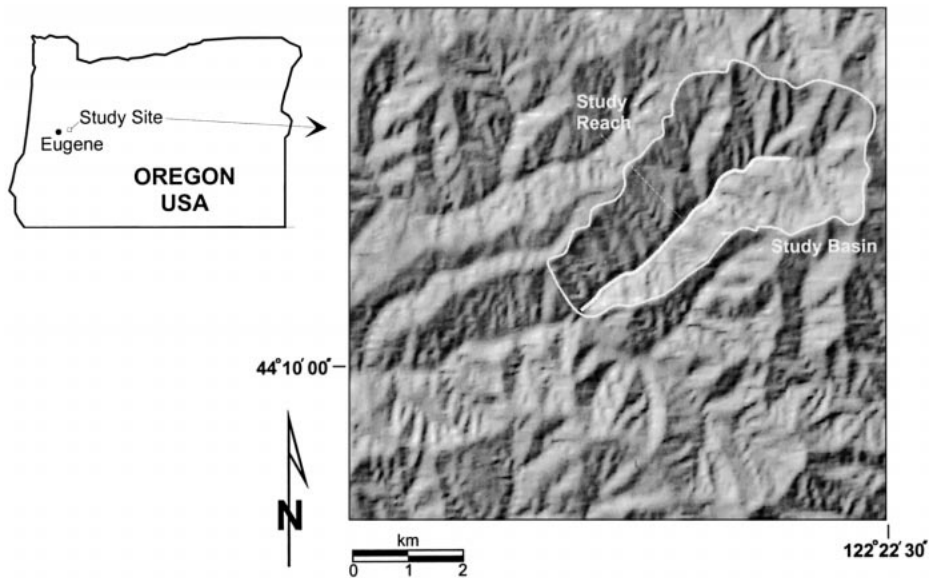


Figure 1. Location map and shaded relief image of the study basin: Gate Creek, Oregon Cascade Range.

the development and movement of sediment waves over entire channel networks (Benda and Dunne, 1997).

Despite field observations, laboratory experiments, and simulation modeling, the geomorphic importance of sediment waves remains poorly understood (Benda and Dunne, 1997; Gomez et al., 1989; Nicholas et al., 1995). One impediment to better understanding is the absence of a definitive set of physical criteria for identifying sediment waves in the field and for interpreting their effects on channel and valley-floor morphologies. In this study we examine the mass-wasting origin and subsequent downstream progression of a sediment wave through a small mountain channel. A series of field measurements document the extent of in-channel deposition and subsequent incision through reaches traversed and currently occupied by the sediment wave at the time of the study. We examine changes in channel form, substrate sizes, and terrace height, and use these measurements to estimate potential bedload transport rates over the wave, from which we infer potential rates of wave movement and mechanisms for maintaining sediment-wave coherency.

STUDY SITE

The South Fork of Gate Creek is in the Cascade Range of west-central Oregon, United States (Fig. 1). Volcaniclastic rocks comprise the dominant lithology. The steep and highly dissected topography has been sculpted by shallow landsliding and debris flows. The av-

erage annual precipitation is >200 cm/yr; more than 70% falls between November and March. Snow accumulates during the winter above ~ 1500 m elevation. The lower part of the study watershed, that below 1000 m elevation, is in the western hemlock vegetation zone. The upper watershed is in the Pacific silver fir zone (Franklin and Dyness, 1973).

The South Fork of Gate Creek has a drainage area of 55 km². The 4.5 km study reach occupies a 15 km² portion of the upper watershed. The third- to fourth-order channel is 10–30 m wide and is confined by steep hillslopes within 10–100-m-wide valley floors. Channel gradients along the study segment range between 7% and 2%.

METHODS

A longitudinal profile was surveyed using auto level and tape along the upper South Fork of Gate Creek (Fig. 1) during low flow over a two week period in October 1996. This survey encompassed the entire channel length that showed signs of fluvial deposition or erosion from the February 1996 storm. The survey included elevations of the channel thalweg and of recently buried flood-plain and terrace surfaces; the average station spacing was 20 m. Channel types along the surveyed reach were noted using the classification of Montgomery and Buffington (1997). We also recorded evidence of valley-floor flooding and deposition, including the locations of side channels and recently buried trees. To document downstream changes in valley and chan-

nel morphologies, 17 across-valley surveys were linked to the longitudinal survey. Figure 2 shows cross-section locations.

Grain-size distributions were estimated with pebble counts (Wolman, 1954) from channel beds and newly deposited alluvial surfaces at each of the cross sections. Pebble counts included at least 100 clasts that had an intermediate axis >2 mm. Clasts of <2 mm were excluded from the analysis. The channel bed exhibited a systematic variation in morphology downstream; there were large local changes in texture through some reaches. Through cascade and step-pool reaches, sampling encompassed a representative reach extending several channel widths downstream. Through pool-riffle and meandering reaches, samples were taken from riffles and point bars. The texture of the riparian surface was relatively uniform at each cross section, so no spatial subsampling of the area was required. Characteristics of the grain-size distributions obtained from these samples, e.g., median diameter, were made directly from the observed frequency-by-number relationships (Kellerhals and Bray, 1971).

OBSERVATIONS: CHANNEL RESPONSES TO MASS WASTING

Aerial photographs taken in 1994, at a scale of 1:12 000, show a closed canopy of deciduous trees obscuring all of the channel, except for the lower part of the study segment (cross sections 3–5), which had a semi-open canopy and a meandering, single-thread channel with gravel bars. The channel through this lower portion is displaced by the distal ends of fans at the mouths of two adjacent, second-order basins. On the basis of 1993 habitat surveys (Oregon Forest Industries Council, 1993), the prestorm channel throughout the study segment was single thread, with a coarse, cobble to cobble-boulder texture and step-pool to pool-riffle morphology.

The nine debris flows triggered by the 1996 storm released an estimated total of 18 000 m³ of coarse sediment and an unknown volume of woody debris into Gate Creek. Visitors immediately after the storm found a continuous set of fluvial terraces, unvegetated and littered with flood debris along ~ 3.5 km of the channel. At many locations, newly deposited sediment buried the bases of streamside trees (Fig. 3). Poststorm 1996 aerial photographs show widening of the channel throughout the study reach to just below cross section 3; there were no apparent storm-induced changes downstream of that point. An area of high sediment storage occupied the downstream one-

third of the study segment during the survey period in the fall of 1996. This aggraded zone was coincident with and extended upstream of the semi-open canopy, meandering reach visible in the 1994 aerial photographs. The downstream portion of this aggraded zone was braided at the time of our survey. The braided reach abutted a logjam formed at a debris-flow entry point. Downstream of the braided reach, the channel appeared unaltered, with a coarse-grained pool-riffle bed and intact riparian vegetation.

The location and approximate volume, excluding fine grain sizes, of the debris flows entering upstream of and along the study reach are shown in Figure 2. Debris-flow volumes were estimated by integrating the field-estimated area of cross-sectional scour over scour length as part of an analysis conducted by the Weyerhaeuser Company (J. Ward, 1996, personal commun.). The exact timing of the individual debris flows during the storm is not known. They occurred within a 24–48 h period during February 6 and 7, 1996 (Ted Turner, Weyerhaeuser Company, 1996, personal commun.), suggesting that there were multiple pulses of sediment delivery to the stream channel.

From these and other observations described in the following, we infer the following sequence of events. Prior to upstream mass wasting, channel morphology was characterized by a boulder- or cobble-dominated step-pool or pool-riffle environment. Several debris flows entered the system at the channel head and inundated the narrow valley floor for several hundred meters downstream. This sediment, augmented with that from additional debris flows entering the channel from downstream tributaries, moved downstream as a relatively coherent sediment wave, or waves, during the concurrent flood. For points downstream, arrival of the sediment wave caused mean grain size of sediment composing the bed to become finer and the channel to aggrade to the level of the adjacent flood plain and terrace. The bases of streamside trees were buried by alluvium. The channel became braided and side channels cut into vegetated riparian areas that, prior to aggradation by the sediment wave, had been forested terraces. Mean grain size of sediment composing the channel bed progressively coarsened as the sediment wave moved on. Eventually, the channel was incised to an immobile substrate; either the previously buried boulder or bedrock bed was exhumed or the channel became armored with a boulder lag. At this point, the channel was inset 1 m or more, confined by alluvial bank material, and characterized by a

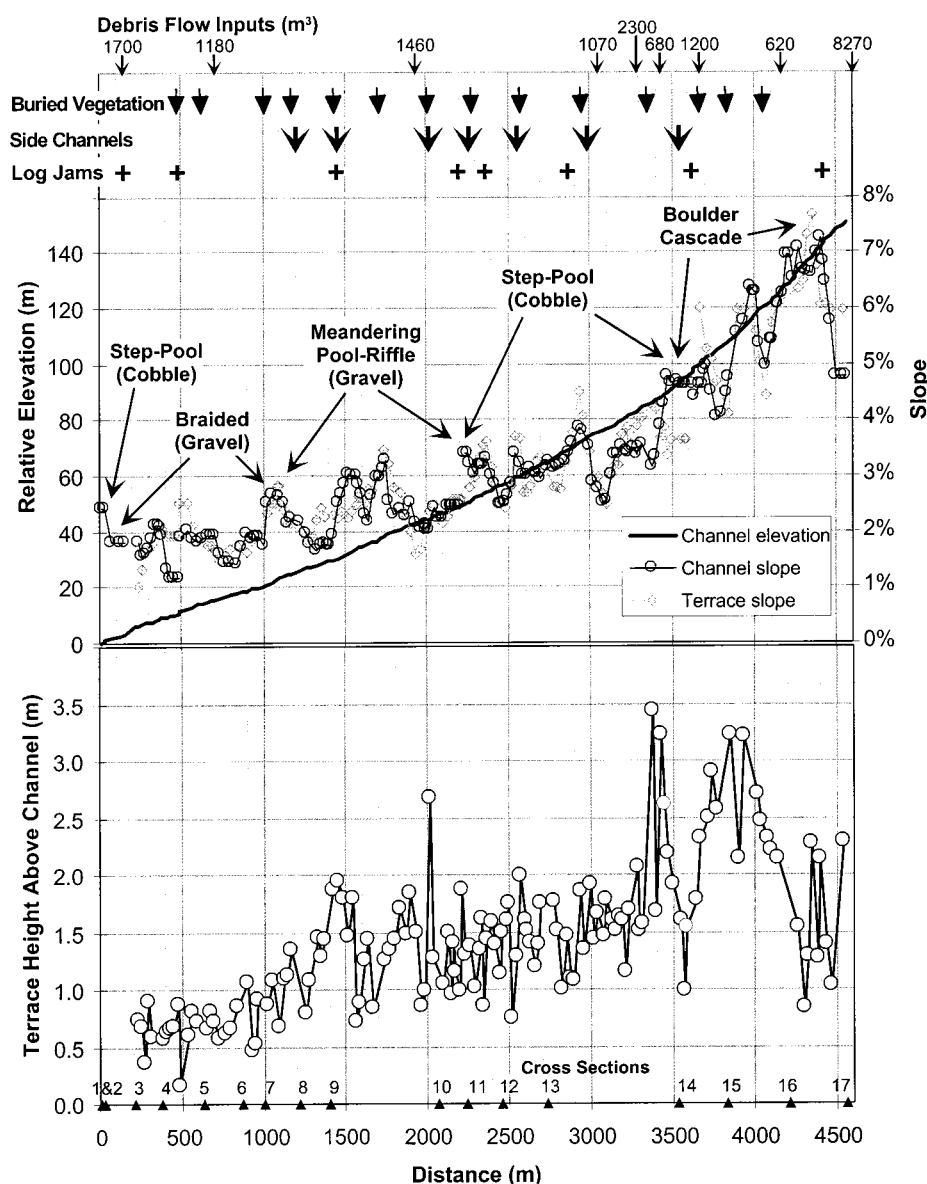


Figure 2. Graphical summary of the channel survey. Channel slopes were estimated from linear regressions of surveyed elevations over a centered 50 m window. The lower graph shows terrace heights along the study reach. Each point represents a location of some change in terrace or channel characteristics (e.g., gradient). Abrupt changes result in closely spaced or coincident points. Locations of logjams, debris-flow inputs, side channels, and buried vegetation are shown by the symbols above. Of the 8 logjams found, only those at 200, 500, 3600, and 4400 m spanned the entire channel width.

step-pool morphology. The valley floor gained a fresh veneer of alluvial gravel, significant woody debris, and numerous abandoned side channels. The aggraded portion of the channel presumably marks the location of the sediment wave at the time of the survey.

Downstream Variation in Terrace Height

The survey shows a general pattern of increasing channel incision upstream (i.e., in-

creasing elevation differences between channels and the newly buried terraces), shown in Figure 2. Channel incision ranged from 2 to 3 m in the upper 1 km of the study segment to <1 m in the lower 1 km. The cross-section profiles, reproduced in Figure 4, clearly show the downstream variation of channel form.

In addition to the downstream trend of decreasing channel incision, the surveys also show significant local along-channel variability in the depth of incision. For example, Fig-



Figure 3. Photograph of channel deeply incised through recently deposited alluvium near cross section 13.

Figure 2 shows the locations of all logjams along the survey reach. Those at ~200, 500, 3600, and 4400 m spanned the entire channel width and had trapped sediment upstream, resulting in lower terrace heights. Although the logjams contributed to along-channel variability in terrace heights, other sources of variations are related to local narrowing of valley floors and transient obstructions, including debris-flow deposits and boulder accumulations. We did not attempt to document the source of reach-to-reach variability of terrace heights.

Particle-Size Distributions on Channels and on Newly Deposited Alluvium

The median particle size (D_{50}) of the channel bed ranged from 170 mm upstream (cross section 13) to 32 mm downstream (cross section 4). The 84th percentile (D_{84}) showed a higher rate of decline, ranging from 260 to 75 mm over the same distance. In contrast, the surface texture of the newly deposited terrace alluvium does not change substantially downstream. The median particle size on the depositional surfaces across all cross sections was <50 mm, and the D_{84} was <75 mm (Fig. 5).

The finer particle sizes on the newly buried terrace surfaces, as compared to the coarse bed texture of the currently incised channels, reflect channel conditions as they existed during the period of aggradation, the particle distribution of the bed at that time being preserved on the uppermost terrace surface. The fining of channel bed sediments during periods of aggradation has occurred elsewhere (Coates and Collins, 1984; Meade, 1985; Roberts and Church, 1986). The closer correspondence in particle size between newly deposited alluvium

and adjacent channel beds in the lower part of the study segment at cross sections 3–7 indicates that those cross sections were aggraded at the time of the survey. The relatively abrupt decline in both the D_{84} and D_{50} of the channel-bed surface beginning at cross section 7 corresponds to the zone of declining terrace height (Fig. 2), reflecting the area of higher sediment storage.

Valley Floor and Channel Morphology

Channel morphology was classified into four categories: (1) braided; (2) meandering pool-riffle; (3) step pool; and (4) boulder cascade (Fig. 2). The boulder-cascade reach was confined to the steepest portion of the channel (5%–7%) above cross section 14 (3500 m). A step-pool morphology dominated between ~2000 and 3500 m (cross sections 10–13), characterized by a coarse substrate consisting primarily of large cobbles (D_{50} <100 mm and a D_{84} <200 mm, Fig. 5). A meandering pool-riffle channel occurred between 2000 m (cross section 10) and 1000 m (cross section 7). The channel was braided over the downstream portion of the study segment, between 250 and 1000 m (cross sections 3–7).

Transitions in stream morphology often correspond to changes in channel gradient (Bisson et al., 1982; Montgomery and Buffington, 1997), as seen here in the transition from a boulder-cascade channel to a step-pool channel at a gradient of ~5%. That part of the study reach through which the gradient varies from only 3% to 2%; however, exhibits three different channel morphologies. These are, progressing from upstream to downstream, step pool, meandering pool-riffle, and braided. These reaches span the transition from the de-

graded to the aggraded channel. The transition from a step pool to meandering pool-riffle channel, occurring between cross sections 12 and 7, corresponds to the transition from low to high in-channel sediment storage, as indicated by the decline in channel incision (Fig. 2) and the fining of the bed sediments (Fig. 5). The transition to braided morphology occurs between cross sections 7 and 3, which corresponds to the zone of least channel incision and finest channel-bed substrate. Relatively fine surface grain sizes (gravel), indicative of high sediment supply, occur on terrace surfaces throughout the study reach.

We found numerous side channels at 1–2 m above the main channel (Fig. 4), the locations of which are plotted in Figure 2. The occurrence of side channels suggests that the channel had a braided morphology at the time of maximum aggradation, similar to the braided morphology in the aggraded reach between cross sections 3 and 7. Channel braiding during periods of channel aggradation has been documented at other sites as well, including the Queen Charlotte Islands (Roberts and Church, 1986) and northern California (Madej and Ozaki, 1996).

Mass Balance: Terrace Genesis by Passage of a Sediment Wave

The channel survey was used to estimate the cumulative volume of sediment excavated from the channel following aggradation, assuming that the channel had initially aggraded to the level of the uppermost paired, newly buried terraces and was incised back to its former bed level. The presence of buried vegetation along freshly exposed channel banks indicated that the channel was not excavated to a width greater than that prior to the storm. To make a continuous estimate of excavated sediment volume along the study segment (cubic meters per meter length of channel), cross-sectional geometry, minus the estimated area of the active channel when aggraded, was interpolated through the intervening reaches. The cross-sectional area of the active channel during the period of aggradation was estimated by fitting channel area as a power function of drainage area over the currently aggraded reach.

These calculations indicate that the cumulative volume of sediment excavated from the study segment is significantly greater than the estimated volume of sediment delivered by debris flows (Fig. 6). This disparity in supplied versus excavated volume suggests that a moving sediment wave (or waves) traversed the upper portion of the study segment. A

downstream-progressing wave can aggrade a limited length of channel and then move on, leaving a continuous record of channel burial. Sediment left on top of existing terraces and flood plains (Fig. 3), which was not included in the estimation of excavated sediment volume, causes an underprediction of the amount of sediment stored along the valley floor.

ANALYSES

Cross-Section Geometry and Discharge Capacity

The extent of aggradation or entrenchment can dramatically affect the flood-carrying capacity of a channel and the frequency of overbank flows. To quantify this effect, we estimated flood magnitudes along the surveyed reach and calculated a rating curve for each cross section. For a given flood discharge, we can then estimate the extent of channel inundation, indicated here using the width/depth ratio and calculated as

$$\frac{w}{\bar{h}} = w^2 A_{cs}, \quad (1)$$

where \bar{h} is mean depth, w is width, and A_{cs} is the cross-sectional area of the wetted channel. Using survey measurements, we can estimate w and A_{cs} as functions of discharge.

A U.S. Geological Survey (USGS) stream gaging station, operated downstream on Gate Creek (drainage area 122 km²) from 1952 until 1990, provides an estimate of flood magnitude. Regional regressions for flood discharge (Harris et al., 1979) indicate that discharge varies almost linearly with drainage area. Hence, we estimate discharge at each cross section using the gage record, normalized by drainage area. Annual peak flows, fit with a Log Pearson Type III distribution, give the flood-frequency relation shown in Figure 7.

A rating curve for each cross section is constructed by estimating discharge for a range of flow depths. For a given depth, cross-sectional area (A_{cs}) and hydraulic radius (R) are calculated from the survey points. The discharge associated with a flow depth h is estimated for each cross section as $Q = A_{cs}u$ using an equation by Hey (1979; see also Bathurst, 1993) for mean flow velocity u :

$$u = 5.62\sqrt{gRS} \log\left(\frac{a'R}{3.5D_{84}}\right). \quad (2)$$

Here $a' = 11.1(R/h_{max})^{-0.314}$, where h_{max} is maximum flow depth at the cross section. Developed for flow over riffles through gravel-

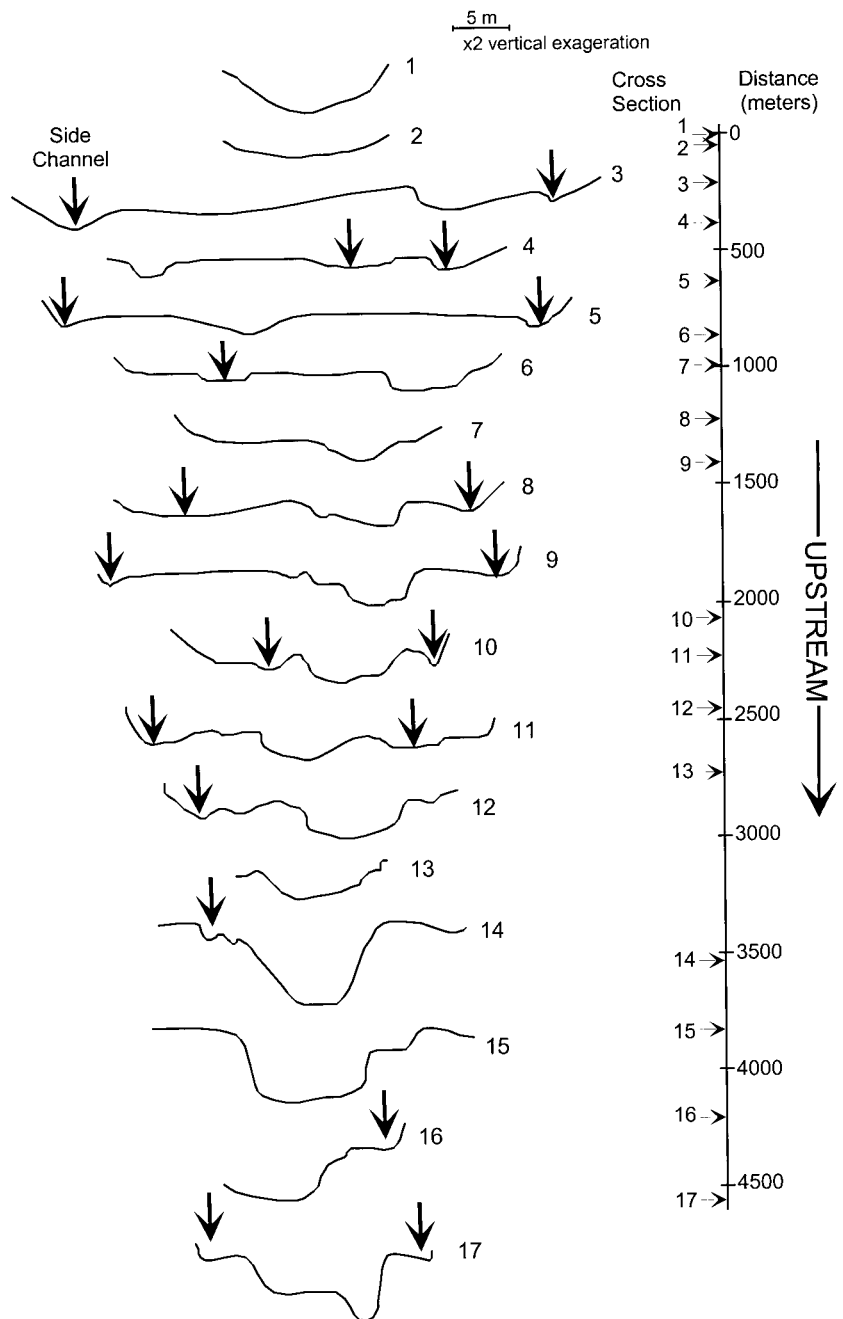


Figure 4. Cross-section geometry (2× vertical exaggeration). Arrows indicate side channels formed during the period of channel braiding. Side channels at cross sections 1–8 are flooded every year; those at cross sections 12–17 are flooded only during extreme flood events.

bedded, pool-riffle reaches, this equation accounts to some extent for the effects of cross-sectional shape.

With equation 1, we calculated a width/depth ratio for each cross section at a variety of flood flows, shown for the 1, 2, and 25 yr flood in Figure 8. The resulting pattern reveals characteristics of channel flood response.

Width/depth ratios between floods of differing magnitudes vary little for upstream reaches. The channel there is sufficiently entrenched to contain even a large flood with no overbank flow. Starting at cross section 7, however, the width/depth ratio increases dramatically between the 1 and 2 yr floods. This pattern is clearly revealed by the difference in width/

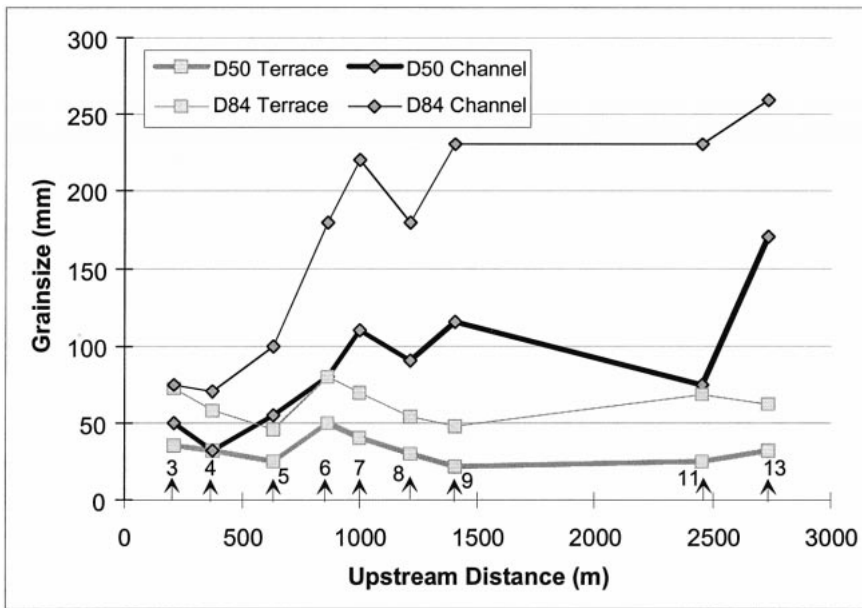


Figure 5. Grain-size characteristics of the channel and terraces.

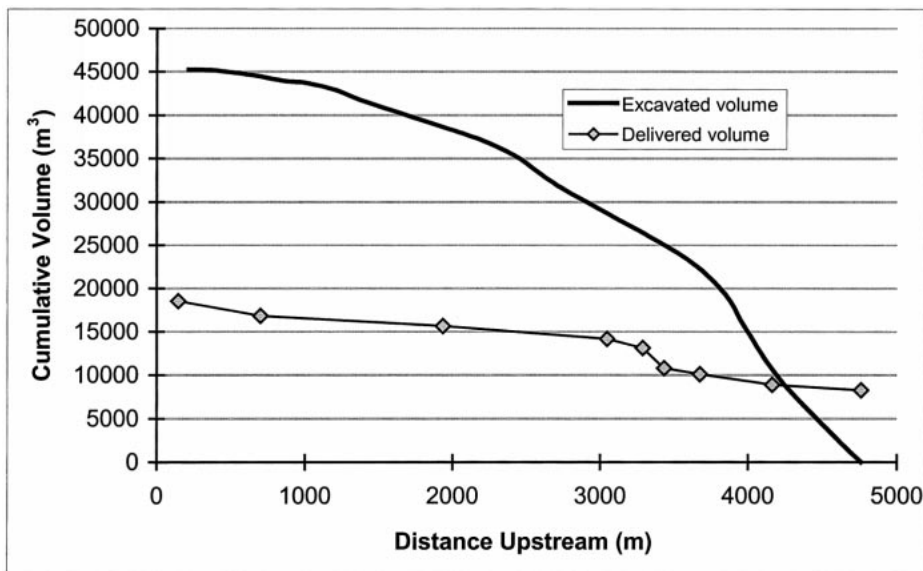


Figure 6. Cumulative volume of sediment delivered by debris flows and cumulative volume of sediment excavated from the channel. Mass balance indicates that the entire reach was not concurrently aggraded.

depth ratio between the 1 and 2 yr floods shown in the lower graph: the change through the lower reaches is positive and large, indicating overbank flow and inundation of the valley floor. The channel there is aggraded and frequently overtopped. Cross sections 1 and 2 show no field evidence of recent aggradation and respond similarly to the upstream, incised channels.

Lack of response to a large-magnitude flood

indicates an entrenched channel, created in this environment through a cycle of aggradation and incision. The valley floor is insulated from the effects of all but the largest floods. A large increase in width/depth ratio between relatively frequent flood magnitudes is indicative of an aggraded reach. The valley floor is frequently flooded. If sediment is excavated from this zone, the channel will incise and discharge capacity will increase. If the sediment

continues downstream as a coherent wave, the zone of valley-floor flooding will accompany it.

Spatial Variation in Bedload Transport: Mechanisms that Maintain a Sediment Wave

Channel morphology and grain-size distribution of both the bed and subsurface provide indicators of bedload transport rates during flood flows in aggraded and incised reaches. Estimates of total bedload flux Q_b as a function of longitudinal channel length offer a means of evaluating future channel changes. We can estimate bedload flux and transport velocity at each surveyed cross section. The downstream variation in calculated flux provides an indication of along-channel variations in erosion and deposition.

To estimate volumetric changes of in-channel stored sediment year to year, we integrate bedload flux over time to estimate the total volume moved through each cross section. This requires a time series of discharge and a bedload-rating curve that relates sediment flux, Q_b , to water flux, Q_w . The USGS Gate Creek gage provides an estimate of discharge. Bedload transport is estimated as described in the following.

Bedload flux is calculated using Parker's (1990a) surface-based transport relation. This equation is particularly useful for our purposes because it uses the grain-size distribution of the channel-bed surface, quantified by pebble counts at selected cross sections. It allows us to use variations in bed-surface texture as indicators of relative transport rate. (We use the transport rates recorded by the bed-surface textures found at summer low flow during the time of the survey. Presumably, these bed textures represent those formed during the last bedload-transporting discharge.) With Parker's equation, bedload flux per unit bed area for size class i is given as

$$q_{si} = W^*(\tau/\rho)^{3/2}(\rho_s/\rho - 1)g f_i \quad (3)$$

The total unit bedload is then $q_s = \sum q_{si}$. Here τ is shear stress at the channel bed, estimated as $\rho g h S$, where ρ is water density, h is flow depth, S is water-surface slope, and g is gravitational acceleration; ρ_s is sediment density; f_i is the proportion by volume of grains in the i th size range contained in the surface layer of the bed; and W^* is a dimensionless bedload transport rate. W^* is calculated as

$$W^* = 0.0025G(\phi), \quad (4)$$

where

$$G(\phi) = 5474 \cdot (1 - 0.853/\phi)^{4.5}, \quad \phi > 1.59; \quad (5)$$

$$G(\phi) = \exp[14.2(\phi - 1) - 9.28(\phi - 1)^2], \quad 1 \leq \phi \leq 1.59; \quad (6)$$

$$G(\phi) = \phi^{1.42}, \quad \phi < 1. \quad (7)$$

Here ϕ is calculated as

$$\phi = \pi \phi_{sg0} g_0(\delta_i), \quad (8)$$

where $\phi_{sg0} = \tau_{sg}^* / \tau_{sg0}^*$, with $\tau_{sg}^* = \tau / \{ \rho [(\rho_s - \rho) / \rho] g D_{sg} \}$, and D_{sg} is the surface geometric mean grain size; $g_0(\delta_i)$ is a hiding function given by $g_0 = \delta_i^{-0.0951}$, where $\delta_i = D_i / D_{sg}$ and D_i is the mean size of the i th size range; and π is a straining parameter shown graphically in Parker (1990a) and tabulated in Parker (1990b). The reach-specific parameters required are water-surface gradient S , flow depth h , and D_{sg} and D_i for the bed-surface grain-size distribution. For a given flow depth, we integrate q_s over the width of the cross section to estimate total bed load, Q_s . Because depth varies over the cross section, q_s is calculated point to point and integrated numerically.

To calculate shear stress τ , we estimate water-surface gradient S from the surveyed channel elevations and set a value for flow depth. Gradient is estimated point by point using a linear regression over all survey points within a 50 m window centered about the point of interest. The channel cross-sectional area A_{cs} and hydraulic radius R for the specified flow depth are calculated from the cross-sectional survey. Discharge is calculated as $Q_w = A_{cs} u$, with mean flow velocity (u) estimated with equation 2. To create a bedload-rating curve, we calculated Q_w and Q_s for a range of flow depths.

It is instructive to normalize the calculated bedload transport rate. As discussed by Bagnold (1973), the energy per unit time available for moving sediment as bedload is some fraction of total stream power Ω , which for steady flow is expressed as

$$\Omega = \rho g Q_w S. \quad (9)$$

To estimate Ω , we approximate S as channel slope and assume that $Q_w \propto$ drainage area, A . Hence, $\Omega \propto AS$, and the quantity AS serves as an indicator of potential sediment transport capacity. Figure 9 shows AS calculated for each surveyed cross section; drainage area is estimated with planimeter from a 1:24 000 scale topographic map. This graph shows how the total bedload transport capacity varies downstream. Actual transport capacity will differ

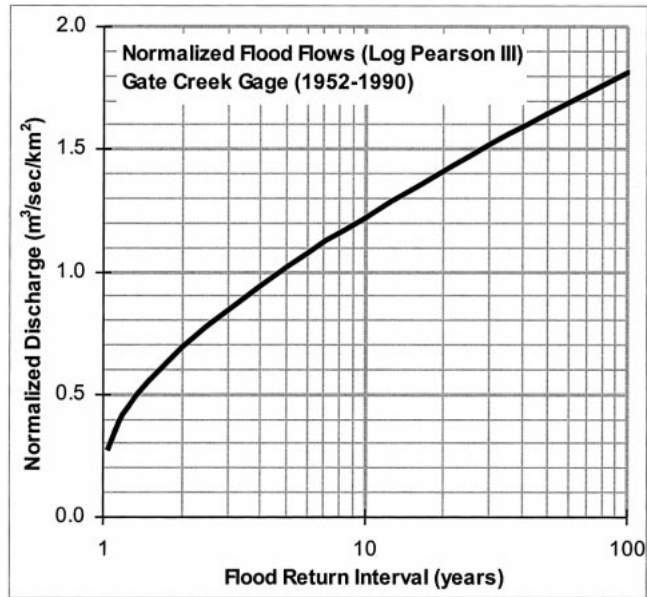


Figure 7. Flood frequency for discharge normalized by drainage area.

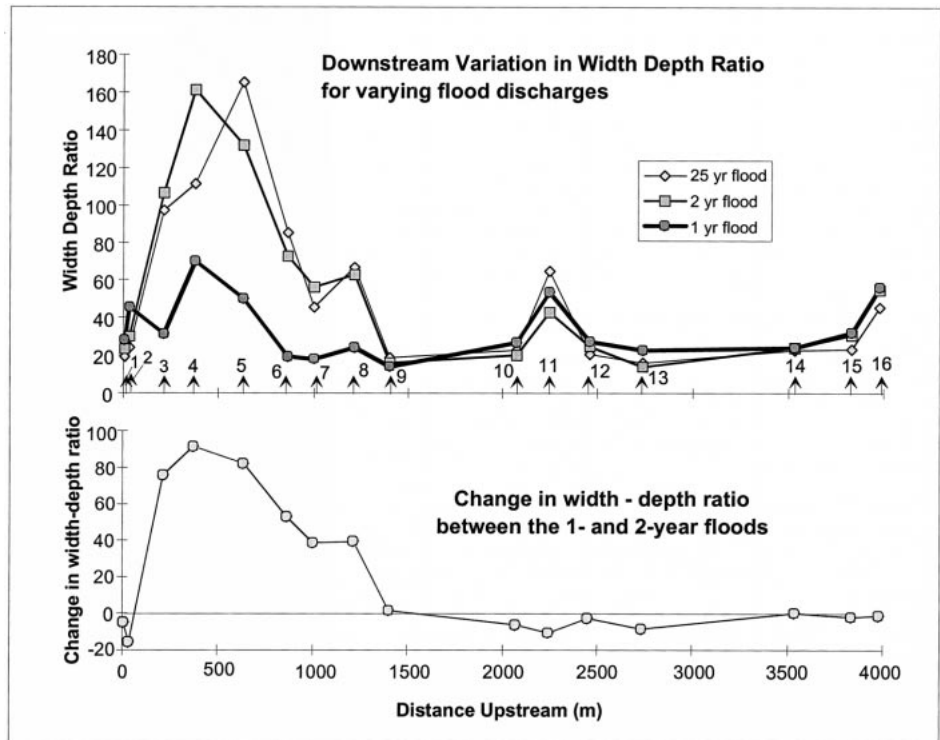


Figure 8. Downstream variation of width-depth ratio for various flood flows. The large variation in this ratio between 1 and 2 yr floods for cross sections 3–8 indicate frequent inundation of the valley floor through the aggraded reach. The relatively constant value at all other cross sections indicates no overtopping of the channel, even for relatively high magnitude, 25 yr recurrence-interval floods.

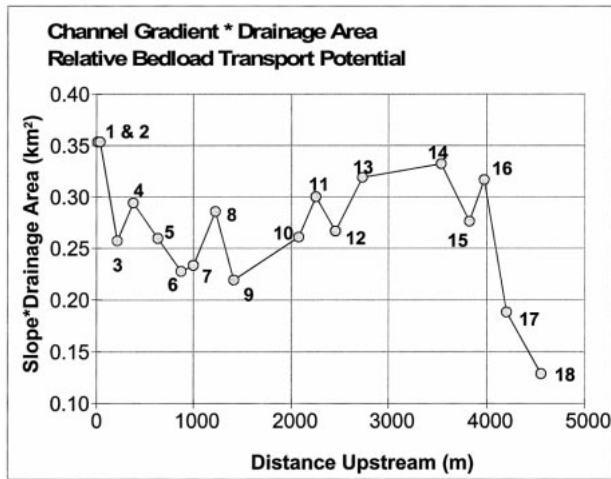


Figure 9. Slope-area product as an indicator of bedload transport potential.

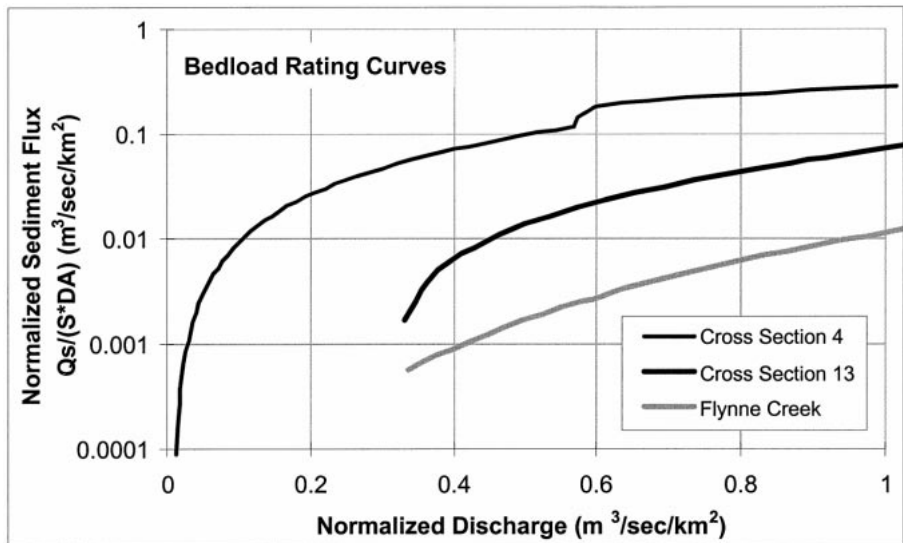


Figure 10. Bedload rating curves for cross sections 4 and 13. Included for comparison is the rating curve reported by Jackson and Beschta (1982) for Flynne Creek, a third-order Oregon Coast Range stream.

from this pattern because of along-channel variations in transport efficiency. Estimates of bedload transport rate, normalized by AS , then provide an indicator of transport efficiency.

Rating curves were calculated for cross sections 1, 3, 4, 5, 6, 7, 8, 9, 11, and 13. Figure 10 shows the bedload rating curves calculated for cross sections 4 and 13. These have the highest and lowest, respectively, total annual transport potential and delineate the envelope of curves for these cross sections. These curves differ in two important aspects. First, transport rates at cross section 4 are from 5 to 10 times greater for a given flood magnitude, even though cross section 4 has a somewhat lower slope-area product (Fig. 9). Second, sig-

nificant transport begins at cross section 4 at a much lower discharge. The greater transport efficiency of cross section 4 results primarily from the lack of surface armoring of the channel bed.

Figure 10 shows the rating curve reported by Jackson and Beschta (1982) for a third-order Oregon Coast Range stream, which for a given discharge indicates bedload transport almost an order of magnitude lower than that estimated for cross section 13. Such discrepancies highlight the difficulties in using general transport relations for estimating bedload discharge in rivers (e.g., Gomez and Church, 1989). We assume for the remaining discussion that all errors are systematic at all cross

sections and that the downstream pattern in relative flux magnitude is correct. It is important to note that these results provide, at best, order-of-magnitude estimates of potential bedload flux rates.

The along-channel variation in transport efficiency is illustrated by using the rating curves with the time series of daily mean discharge to calculate cumulative annual bedload transport. Figure 11 shows the annual frequency distribution of mean daily flows, normalized by drainage area. Comparison with the bedload rating curves shows that transport at cross section 4 is predicted to occur over a substantial portion of most years (more than six weeks), whereas no transport at all is predicted in low-flow years for cross section 13.

Figure 12 shows annual transport volumes. These values indicate dramatic along-channel variation in transport efficiency. Large transport volumes are predicted at cross sections 3, 4, and 5. These cross sections are located along the downstream portion of the aggraded reach. Bed texture and channel morphology through this zone indicate much larger transport rates than those upstream and downstream.

The increase in apparent bedload transport over the downstream portion of the aggraded reach is primarily a consequence of the smaller average grain size of the surface layer of bed sediment through this zone. As shown in Figure 5, pebble counts of the surface layer indicate that D_{50} and D_{84} decrease substantially at these cross sections. Grain size of the bed surface layer coarsens downstream of the log-jam below cross section 3; D_{50} and D_{84} values at cross sections 1 and 2 are similar to those found at cross section 13. These variations in bed-surface texture correlate with variations in cross-sectional geometry, as illustrated by the width/depth ratio in Figure 9. The lack of well-developed surface armor and the highest bedload transport rates are found at the most aggraded cross sections, i.e., those having the most in-channel sediment available to be moved.

Sediment-Wave Propagation

These observations indicate high rates of bedload transport through aggraded reaches, as shown for the terraces and at cross section 4. As sediment delivery from upstream wanes, the channel-filling sediment is excavated, the channel incises, transport rates decrease, and the bed surface coarsens. Estimated transport rates suggest that the entire volume of delivered sediment can be flushed through the channel relatively quickly. Much of the deliv-

ered sediment was moved several kilometers through the channel (by a large flood event) over the course of a single season. Much of that sediment now occupies ~1 km of the channel upstream of the logjam below cross section 3. This interpretation suggests that, as the channel moves sediment around or through the logjam during subsequent floods, the sediment wave will progress downstream.

Using estimates of bedload transport velocity estimated from particle tracer studies, we can use the rating curves to estimate rate and distance of transport of the sediment wave. Hassan et al. (1992) examined numerous tracer studies and found a rough correlation between virtual transport velocity (V_b) and excess unit stream power (total stream power per unit width, $\omega = \tau u$, minus the stream power at which bedload transport begins, ω_0):

$$V_b = 0.0192(\omega - \omega_0), \quad (10)$$

using Bagnold's (1980) estimate of ω_0 ,

$$\omega_0 = 290D_{50}^{1.5}\log(12h/D_{50}). \quad (11)$$

Assuming unlimited supply and unchanging conditions downstream, equation 10, coupled with the time series of discharge and bedload rating curves, can be used to calculate a travel distance for all sediment passing any cross section over the course of a water year. Figure 13 shows the downstream distribution of this sediment for cross sections 1, 4, and 6. These calculations suggest that, even over the course of a low-flow year, all the upstream delivered sediment (~18 000 m³) could be transported through cross section 4 and deposited over a broad length of channel extending kilometers downstream. (It is interesting to note that a factor of 10 decrease in predicted transport rates, as shown by the Flynne Creek rating curve in Figure 10, brings the total volume flux past cross section 4 during the high-flow year of record directly in line with the total volume of sediment delivered from upstream during the flood of 1996.) These results, however, assume unlimited sediment supply. As sediment is excavated from the channel, the surface layer of bed sediment becomes coarser, thus armoring the bed, with a consequent reduction in transport rates and distances. Likewise, sediment deposited in downstream reaches must first aggrade the channel and reduce average grain size of the surface layer before such high rates of transport are attained. Transport rates and annual transport distances are very high over the sediment wave, but decrease dramatically upstream and downstream.

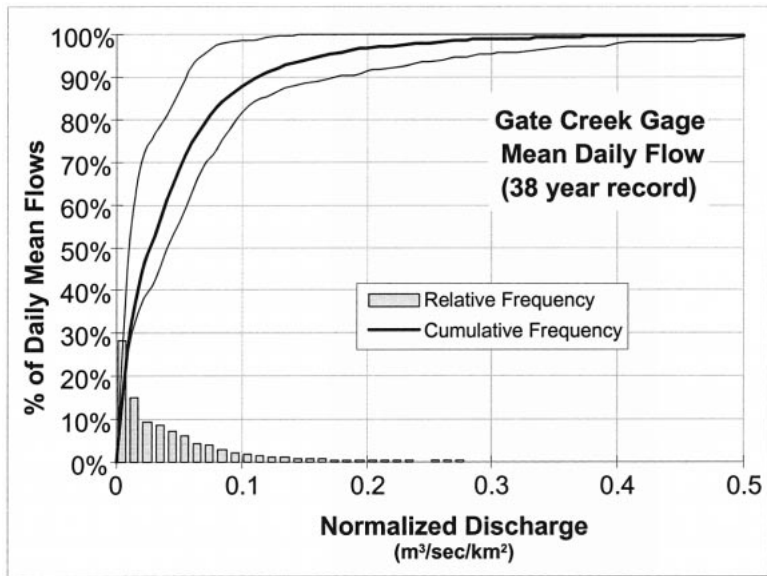


Figure 11. Frequency distribution of annual mean daily discharge, normalized by drainage area (m³/s/km²). The thick solid line shows the cumulative distribution for the mean daily discharge; thinner lines show cumulative distributions for the low-flow (upper line) and high-flow (lower line) years of record.

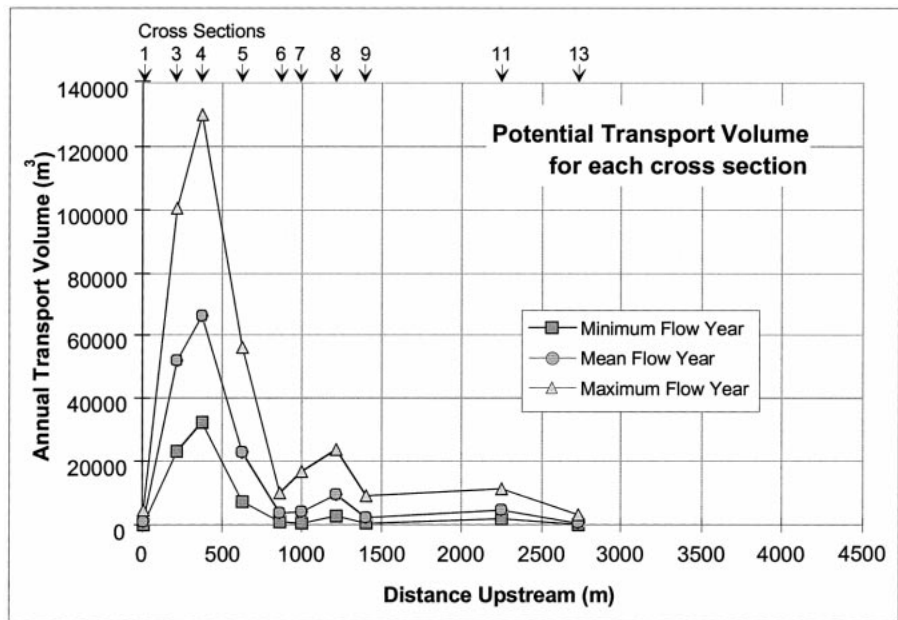


Figure 12. Total annual volume of bedload transport for cross sections 1–13. These values represent integration of the rating curves in Figure 10 by the time series of discharge estimated for each cross section from the Gate Creek gage. Calculations are shown for maximum, minimum, and mean flow years.

Figure 13 shows that variation in bedload transport rates associated with variable discharge over time causes sediment carried past a cross section to be deposited through a downstream-tapering wedge. This effect would act to rapidly disperse a sediment wave.

Concurrently, the rapid change in transport rate over the wave, particularly the very rapid decrease in transport downstream of the wave, would act to maintain its coherency. A large, negative downstream gradient in transport velocity, as indicated between cross section 4

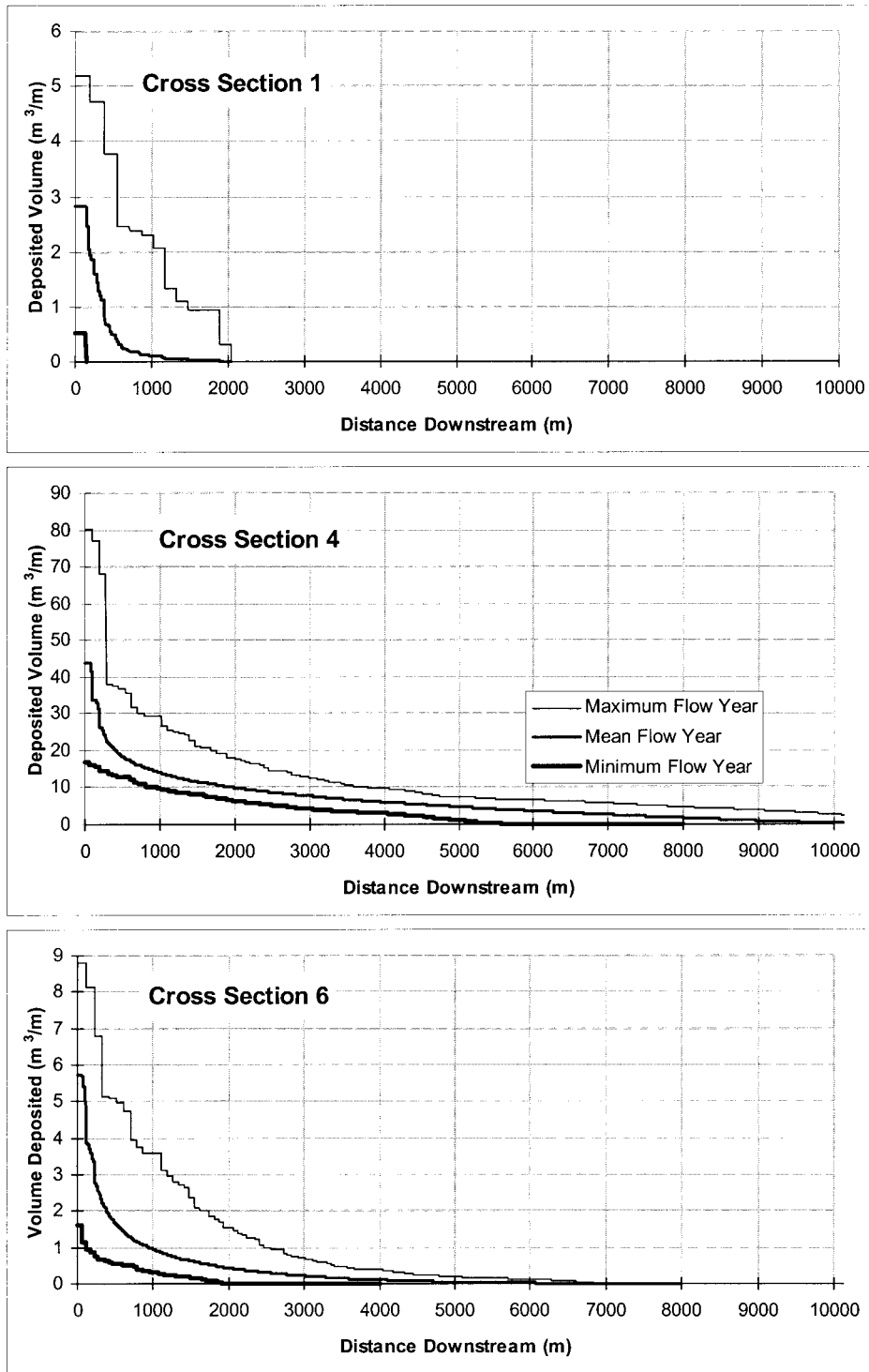


Figure 13. Downstream deposition for sediment transported across cross sections 1, 4, and 6. Note change in vertical scales. The volume transported is calculated with equation 3; the distance traveled is calculated with equation 10. The resulting pattern is determined by integrating both equations over the time series of daily discharge for the maximum-, minimum-, and mean-flow water years. For these calculations, bed texture and channel geometry were assumed unchanged downstream of the cross section.

and cross section 1 downstream, could create a distinct shock-like wave front. Arrival of the front would produce rapid channel aggradation with accompanying widening of the active channel and reduction in the average grain size of sediment composing the surface of the channel bed. Its passage would leave renewed terrace surfaces and an incised channel. As transport rates decrease over the tail of the wave and during waning flood flow, the bed surface may coarsen, as seen in aggraded cross sections 6, 7, and 8. Armoring of the bed surface may limit bedload transport during lower flood flows and effectively freeze a portion of the wave in place, until a flood of sufficient magnitude breaks the armor and re-initiates transport.

Discussion: Factors Affecting Formation and Life of a Sediment Wave

A variety of fluvial processes affect development and downstream propagation of a sediment wave through channels that otherwise carry a much lower sediment load. (1) Channel morphology and bed texture adjust to accommodate vast changes in sediment supply. A large pulse of sediment can be carried through the channel as a large wave, rather than being metered out in small doses. The sediment wave brings with it associated changes in channel form and bed texture. The spatial and temporal extents of this pulse depend in part on the timing of sediment inputs to the channel and on the velocity with which sediment is carried downstream. (2) The sharp transition in sediment-transport velocity over the front of a sediment wave acts to maintain wave coherency by creating a sharp wave front. This change in transport velocity is caused by a large transition in bed-surface texture. (3) Variable discharge over time (e.g., waning flood flow) acts to disperse the wave by smearing sediment into a long downstream-tapering wedge. (4) Coarsening of the bed over the sediment wave as transport rates diminish during waning flood flow may limit or preclude bedload transport during future smaller floods, acting to slow downstream propagation of the sediment wave.

Several other factors not examined in this analysis also affect sediment-wave propagation. Sediment-wave-induced changes in water velocity and depth (e.g., Lisle et al., 1997) affect spatial variation in transport rate, potentially acting to disperse a sediment wave. Travel distances of individual clasts vary widely during bedload-transporting events, also causing sediment-wave dispersion (Nicholas et al., 1995). Widening of the valley floor

will attenuate a sediment wave; overbank deposition and deposition upstream of debris jams will deplete the wave. Numerous interacting processes govern the formation and behavior of sediment waves and, thereby, the effects of sediment influxes on stream channels. The stochastic nature of many of these processes (e.g., the timing of sediment inputs) confounds precise prediction of these effects, thus making the record left by past events extremely valuable in assessing potential impacts of future sediment influxes.

CONCLUSIONS

Sediment supply to streams in landscapes subject to landsliding and debris flows may be characterized by long periods of relatively low sediment input punctuated by brief periods of extremely high input. Although massive influxes of mass-wasting sediment are infrequent, they leave a lasting legacy on valley-floor and channel morphology. At Gate Creek, debris-flow influx created a sediment wave that traveled several kilometers downstream during subsequent flood flow(s). Arrival of the sediment wave caused aggradation and braiding of the channel, reduction in average grain size of sediment clasts composing the surface of the channel bed, and burial of riparian zones. Its passage left a channel incised to a coarse, immobile bed inset between terraces cut by numerous, shallow side channels. Alluvial terraces as high as several meters are ubiquitous in mountain channel networks throughout the Pacific Northwest and the conditions that created them here occur in mountain terrains worldwide. Although terraces are created by a variety of processes (incision of fans, deposition behind debris jams), our analysis at Gate Creek suggests that contemporaneous terraces extending along kilometers of bedrock or boulder-bedded channel record the passage of mass-wasting-initiated waves of sediment. The terraces provide a measure of potential mass-wasting impacts to stream channels and valley floors.

ACKNOWLEDGMENTS

We thank Ted Turner, Weyerhaeuser Timber Company, who introduced us to Gate Creek and was very helpful with logistical support. We also thank Giustina Land and Timber for allowing us to conduct this study on their property. John Burke, Brooke Stewart, and Joan Sias contributed substantially to the conduction of the channel survey. This work was funded with a grant from the National Council for Air and Stream Improvement; thanks to Walt Megahan and Kate Sullivan for their assistance

in this endeavor. Our presentation of this material benefited from review comments by Lisa Ely, Gerilyn Soreghan, and Ellen Wohl.

REFERENCES CITED

- Bagnold, R.A., 1973, The nature of saltation and of 'bedload' transport in water: Royal Society of London Proceedings, ser. A, v. 332, p. 473-504.
- Bagnold, R.A., 1980, An empirical correlation of bedload transport rates in flumes and natural rivers: Royal Society of London Proceedings, ser. A, v. 372, p. 453-473.
- Bathurst, J.C., 1993, Flow resistance through the channel network, in Beven, K., and Kirkby, M.J., eds., Channel network hydrology: New York, Wiley, p. 69-98.
- Benda, L., and Dunne, T., 1997, Stochastic forcing of sediment routing and storage in channel networks: Water Resources Research, v. 33, p. 2865-2880.
- Beschta, R.L., 1981, Patterns of sediment and organic-matter transport in Oregon Coast Range streams, in Proceedings, Symposium on Erosion and Sediment Transport in Pacific Rim Steeplands: International Association of Hydrological Sciences Publication 132, p. 179-188.
- Beschta, R.L., 1984, River channel response to accelerated mass soil erosion, in O'Loughlin, C.L., and Pearce, A.J., eds., Proceedings, Symposium on Effects of Forest Land Use on Erosion and Slope Stability: Honolulu, Hawaii, East-West Center, p. 155-164.
- Bisson, P.A., Nielsen, J.L., Palmason, R.A., and Grove, L.E., 1982, A system of naming habitat types in small streams, with examples of habitat utilization by salmonids during low streamflow, in Armantrout, N.B., ed., Acquisition and utilization of aquatic habitat inventory information: Portland, Oregon, Western Division, American Fisheries Society, p. 62-73.
- Coates, R., and Collins, L., 1984, Streamside landsliding and channel change in a suburban forested watershed: Effects of an extreme event, in O'Loughlin, C.L., and Pearce, A.J., eds., Proceedings of Symposium on Effects of Forest Land Use on Erosion and Slope Stability: Honolulu, Hawaii, East-West Center, p. 155-164.
- Everitt, B.L., 1968, Use of cottonwood in an investigation of the recent history of a floodplain: American Journal of Science, v. 266, p. 417-439.
- Franklin, J.F., and Dyrness, C.T., 1973, Natural vegetation of Oregon and Washington: Portland, Oregon, Pacific Northwest Forest and Range Experimental Station, USDA Forest Service Technical Report PNW-84, 417 p.
- Gilbert, G.K., 1917, Hydraulic-mining debris in the Sierra Nevada: U.S. Geological Survey Professional Paper 105, 154 p.
- Gomez, B., and Church, M., 1989, An assessment of bed load sediment transport formulae for gravel bed rivers: Water Resources Research, v. 25, p. 1161-1186.
- Gomez, B., Naff, R.L., and Hubbell, D.W., 1989, Temporal variations in bedload transport rates associated with the migration of bedforms: Earth Surface Processes and Landforms, v. 14, p. 135-156.
- Griffiths, G.A., 1979, Recent sedimentation history of the Waimakariri River, New Zealand: New Zealand Journal of Hydrology, v. 18, p. 6-28.
- Hack, J.T., and Goodlett, J.C., 1960, Geomorphology and forest ecology of a mountain region in the central Appalachians: U.S. Geological Survey Professional Paper 347, 66 p.
- Harris, D.D., Hubbard, L.L., and Hubbard, L.E., 1979, Magnitude and frequency of floods in western Oregon: U.S. Geological Survey Open-File Report 79-533, 29 p.
- Hassan, M.A., Church, M., and Ashworth, P.J., 1992, Virtual rate and mean distance of travel of individual clasts in gravel-bed channels: Earth Surface Processes and Landforms, v. 17, p. 617-627.
- Hey, R.D., 1979, Flow resistance in gravel-bed rivers: American Society of Civil Engineers, Journal of the Hydraulics Division, v. 105, p. 365-379.
- Jackson, W.L., and Beschta, R.L., 1982, A model of two-phase bedload transport in an Oregon Coast Range stream: Earth Surface Processes and Landforms, v. 7, p. 517-527.
- James, L.A., 1991, Incision and morphologic evolution of an alluvial channel recovering from hydraulic mining sediment: Geological Society of America Bulletin, v. 103, p. 723-736.
- Janda, R.J., Nolan, K.M., Harden, D.R., and Colman, S.M., 1975, Watershed conditions in the drainage basin of Redwood Creek, Humboldt County, California, as of 1973: U.S. Geological Survey Open-File Report 75-568, 257 p.
- Kellerhals, R., and Bray, D.I., 1971, Sampling procedures for coarse fluvial sediments: American Society of Civil Engineers, Journal of the Hydraulics Division, v. 97, p. 1165-1179.
- Kochel, R.C., Ritter, D.F., and Miller, J., 1987, Role of tree dams in the construction of pseudoterraces and variable geomorphic response to floods in Little River Valley, Virginia: Geology, v. 15, p. 718-721.
- Lisle, T.E., Pizzuto, J.E., Ikeda, H., Iseya, F., and Kodama, Y., 1997, Evolution of a sediment wave in an experimental channel: Water Resources Research, v. 33, p. 1971-1981.
- Madej, M.A., and Ozaki, V., 1996, Channel response to sediment wave propagation and movement, Redwood Creek, California, USA: Earth Surface Processes and Landforms, v. 21, p. 911-927.
- Meade, R.H., 1985, Wavelike movement of bedload sediment, East Fork River, Wyoming: Environmental Geology and Water Science, v. 7, p. 215-225.
- Montgomery, D.R., and Buffington, J.M., 1997, Channel-reach morphology in mountain drainage basins: Geological Society of America Bulletin, v. 106, p. 596-611.
- Nakamura, F., 1986, Chronological study on the torrential channel bed by the age distribution of deposits: Hokkaido University College of Experimental Forestry Research Bulletin, v. 43, p. 1-26.
- Nicholas, A.P., Ashworth, P.J., Kirkby, M.J., Macklin, M.G., and Murray, T., 1995, Sediment slugs: Large-scale fluctuations in fluvial sediment transport rates and storage volumes: Progress in Physical Geography, v. 19, p. 500-519.
- Oregon Forest Industries Council, 1993, Aquatic inventory pilot project, draft stream report to Oregon Forest Industries Council: Salem, Oregon, 44 p.
- Parker, G., 1990a, Surface-based bedload transport relation for gravel rivers: Journal of Hydraulic Research, v. 28, p. 417-436.
- Parker, G., 1990b, The "ACRONYM" series of PASCAL programs for computing bedload transport in gravel rivers, St. Anthony Falls Hydraulic Laboratory External Memorandum No. M-220: Minneapolis, University of Minnesota, 124 p.
- Pickup, G.R., Higgins, R.J., and Grant, I., 1983, Modeling sediment transport as a moving wave—The transfer and deposition of mining waste: Journal of Hydrology, v. 60, p. 281-301.
- Roberts, R.G., and Church, M., 1986, The sediment budget in severely disturbed watersheds, Queen Charlotte Ranges, British Columbia: Canadian Journal of Forest Research, v. 16, p. 1092-1106.
- Sigafoos, R.S., 1964, Botanical evidence of floods and flood-plain deposition: U.S. Geological Survey Professional Paper 485A, 35 p.
- Turner, T.R., 1995, Geomorphic response of the Madison River to point sediment loading at the Madison Slide, southwest Montana [Master's thesis]: Bozeman, Montana State University, 99 p.
- Weir, G.J., 1983, One-dimensional bed wave movement in lowland rivers: Water Resources Research, v. 19, p. 627-631.
- Wolman, M.G., 1954, A method of sampling coarse bed material: Eos (Transactions, American Geophysical Union), v. 35, p. 951-956.

MANUSCRIPT RECEIVED BY THE SOCIETY FEBRUARY 18, 1999
REVISED MANUSCRIPT RECEIVED SEPTEMBER 15, 1999
MANUSCRIPT ACCEPTED NOVEMBER 15, 1999

Printed in the USA